SAE TECHNICAL PAPER SERIES

2001-01-1826/4247

Scavenge Loss Mechanisms and Their Driving Forces in Loop-Scavenged High-Performance Two-Stroke Engines

H. Rosskamp, A. Klimmek and P. Pretzsch
Andreas STIHL AG & Co.

M. Mugele
University of Karlsruhe

The Engineering Society For Advancing Mobility Land Sea Air and Space
INTERNATIONAL

Small Engine Technology Conference and Exhibition
Pisa, Italy
November 28-30, 2001

400 Commonwealth Drive, Warrendale, PA 15096-0001 U.S.A. Tel: (724) 776-4841 Fax: (724) 776-5760 Web: www.sae.org

GLOBAL MOBILITY DATABASE

All SAE papers, standards, and selected books are abstracted and indexed in the Global Mobility Database

ISSN 0148-7191

Printed in USA

2001 01 1826/4247

SCAVENGE LOSS MECHANISMS AND THEIR DRIVING FORCES IN LOOP-SCAVENGED HIGH-PERFORMANCE TWO-STROKE ENGINES

H. Rosskamp, A. Klimmek, P. Pretzsch

Andreas STIHL AG&Co., Waiblingen, Germany

M. Mugele

University of Karlsruhe, Germany

Abstract: To fulfill the forthcoming EPA and CARB emission legislations for handheld outdoor power equipment, strong efforts are undertaken to reduce the high hydrocarbon emissions of two-stroke engines. This is due to the fact that the two-stroke engine has a much better power-to-weight ratio than a mini-four-stroke engine. The research focuses on the one hand into the development of new two-stroke technologies such as charge stratification or compression wave injection for example. On the other hand there is still a significant potential in improving the scavenging process of the conventional Schnürle-scavenged two-stroke engine.

This paper focuses into the analysis of the internal flow behavior of the Schnürle-typ scavenge flow in a 64 cm³ high-performance two-stroke engine for hendheld products. The flow analysis is conducted by means of transient 3D-CFD calculations that are based on experimental data. A newly developed postprocessing approach allows for a detailed analysis of different loss paths during scavenging. The results show that four distinguished loss mechanisms exist: Direct mixture short-circuiting, late loop losses, central mixing losses and near-wall secondary flow losses. These four loss mechanisms are quantified in their contribution to the overall losses and the driving mechanisms are outlined. The newly identified secondary flow path carries a quantity of hydrocarbon losses as significant as direct mixture short-circuiting.

Introduction: Due to its simple construction, compactness, low cost and superior performance, small two-stroke engines are widely used for high-performance outdoor power equipment such as brush cutters, blowers, hedge trimmers and chain saws. The high hydrocarbon emissions from conventional two-stroke engines make it necessary to find ways to reduce the scavenge losses.
Apart from the manufacturers' goal to continuously improve the engines to reduce the emissions and increase fuel economy, new and very stringent exhaust emission regulations have put additional pressure on the development of new engine concepts. STIHL advanced engine technology research is now for several years looking into new ways to reduce the overall engine out raw emissions as a basis for catalyst techniques or airhead scavenging for example to be applied.

Commonly, two basic loss mechanisms are named: mixture short-circuiting and loop scavenge losses (early and late scavenge losses). Also it is known that a major quantity of the losses may be attributed to undefinable mixing of fresh and old charge during scavenging [Blair 1996, Sawada et al. 1998]. The target of the work undertaken within the scope of this paper is to understand the scavenging process in more detail to find new approaches for reducing the emissions.
During an initial steady flow simulation of different cylinder designs, it became evident that there seems to exist a path not described before that feeds rich mixture to the exhaust in the near wall region.

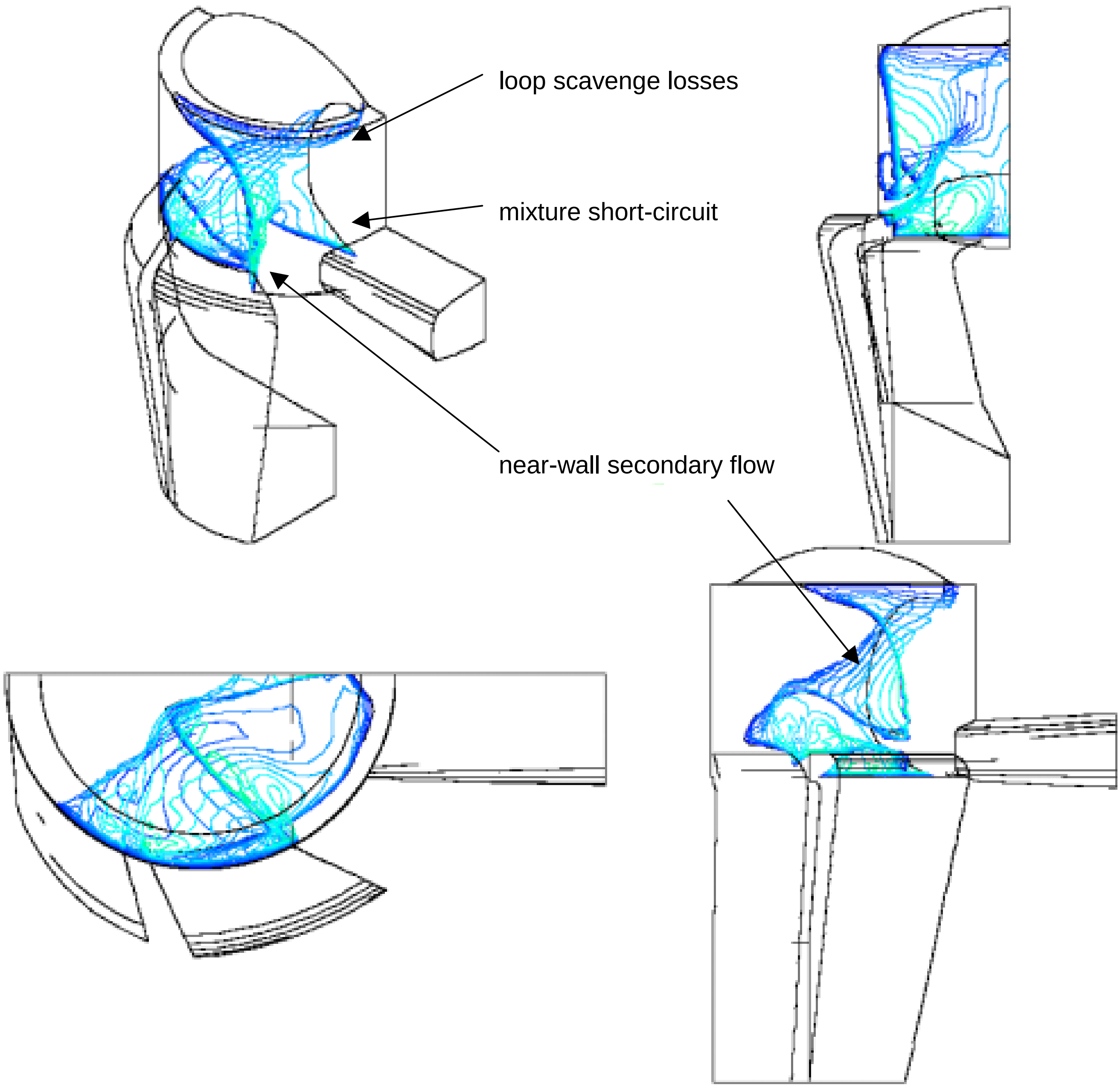

Figure 1: Internal scavenge flow in a generic four-port two-stroke cylinder predicted by a steady flow simulation

Figure 1 shows the iso-surface (fuel concentration) for a given residual concentration at one time-step during the scavenging process. It gives an impression, how the scavenge streams move through the cylinder. Loop scavenge losses and mixture short-circuiting are well known. But also in any calculation a near-wall secondary flow appears. Starting from the wall opposite of the exhaust port, fresh charge moves to the top and side of the cylinder and ends its way by coming down between transfer port and exhaust port. Then this scavenge stream feeds rich mixture into the exhaust. This effect is present in flow predictions with stationary flow as well as in the more precise transient simulation with sliding mesh.

Therefore it was decided to look more detailed into the quantitative contribution of this effect and the driving forces by means of transient flow calculations based upon experimental baseline tests.

Base Engine: Basis for the investigation is a STIHL two-stroke engine of 64 cm³. It has a four-port cylinder (Figure 2). The engine is designed for a rated speed of 9000 rpm giving a 3.2 kW power output. The performance data are listed in Table 1.
This engine has a state-of-the-art design that allows for a good trapping efficiency of about 79%. Therefore, it was decided that this transfer port geometry with flat port roofs is suitable for a detailed analysis of the different scavenge loss mechanisms.

Displacement	64 cm³
Cylinder type	Four finger port
Power	3.2 kW
Rated speed	9000 rpm
HC emission (dyno)	95 g/kWh*
NO_X emission (dyno)	2.5 g/kWh*
CO setting	4.0%

Table 1: Performance data of prototype engine studied (wot-emissions only, rated speed)*

Figure 2: Bottom view of the STIHL 64 cm³ four-port cylinder

Approach: To identify the different flow pattern and scavenge loss mechanisms, a combined approach of 1D- and 3D-CFD simulation is chosen. According to the flow images from the steady flow simulation, balance cells are introduced to identify the origin of the fuel losses (Figure 3).
The balancing sections are defined to form a rectangular block covering the exhaust port of the cylinder with an edge length of 1/6 of the cylinder bore in mid-plane, and the remaining edges corresponding to the maximum dimensions of the outlet orifice. The balanced HC mass fluxes can then be assigned to four different scavenge loss mechanisms: Direct mixture short-circuiting (short-circuiting between near-exit transfer ports and the lower central balance cell surface), late loop (or “Schnürle-“) scavenge losses (entering from the top balance surface into the exhaust), near-wall secondary losses (entering through the side balance surface) and a remaining portion of undefinable central mixing losses (entering through the upper central balance surface) as shown in Figure 3. The mass fluxes over each of these balance cells surfaces are monitored and postprocessed as integrated mass flow for a given crank angle or delivery ratio.

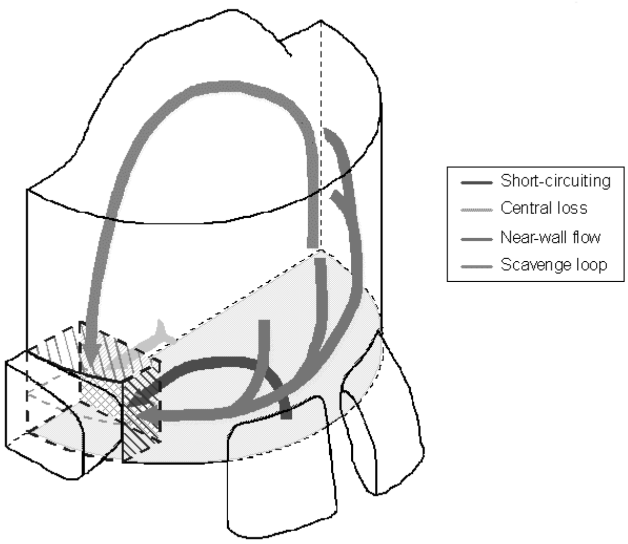

Figure 3: Setup of balance cell surfaces and loss mechanisms assigned to these surfaces

CFD modeling: Target of the CFD study is to mirror the internal flow pattern of the scavenging flow very close to reality. This is indispensable in order to find new ways for reducing raw emissions of the engine. To provide insight into the flow in the cylinder, the cylinder including transfer ports and the attaching part of the crankcase are modeled and calculated using the finite-volume computational fluid dynamic package STAR CD [Star 1997, Mugele et al. 2001]. The boundary conditions are based upon dyno data. The missing data are derived from 1D-simulations using the program Boost. Figure 4 shows the computation grid for the flow simulations. The grid consists of 124,000 nodes and requires 30 h of CPU time on a workstation to calculate the scavenge cycle from 90° a.t.d.c. to 270° a.t.d.c. As the geometry is basically fully symmetric, only a half-model is calculated. The code uses a standard-k-ε-model to describe the turbulent viscosity. The calculation is performed at 9000 rpm which is rated speed of the engine under consideration.

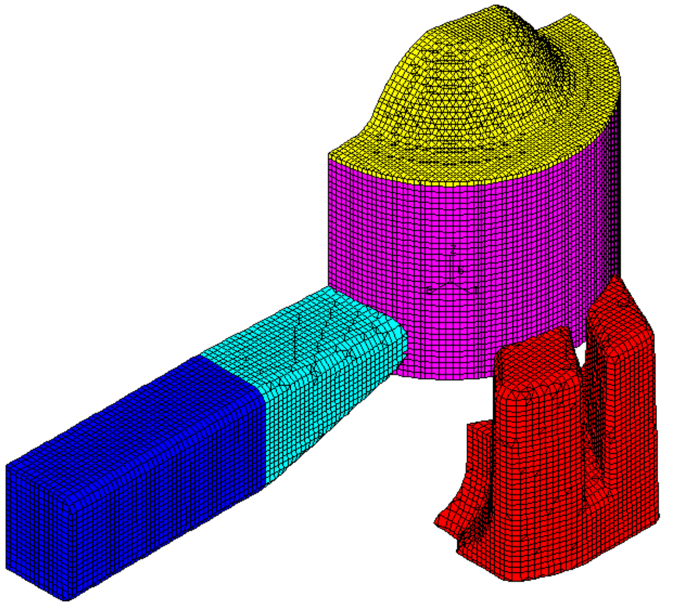

Figure 4: Computation grid used for flow simulation

Validation: To ensure the correctness of the flow simulation, the CFD results are checked against experimental data. The HC trapping efficiency is measured on the test bench resulting in 79% at 9000 rpm. The calculation yields a trapping efficiency of 79% at almost identical mass flux through the engine of 19.8 kg/h, too.
The flow field in the area near the transfer ports and opposite to the exhaust over the piston was checked against flow fields in the real engine assembly obtained by oil paint images and by deposit images from a piston from a fired engine. A typical results is shown in Figure 5. The area near the transfer ports is regarded to be significant for the origin of scavenge streams contributing to the scavenge losses. Since the calculated flow field matches the flow indications from the experiment very well, it is concluded that the CFD predictions are qualitatively correct compared to the real flow field.

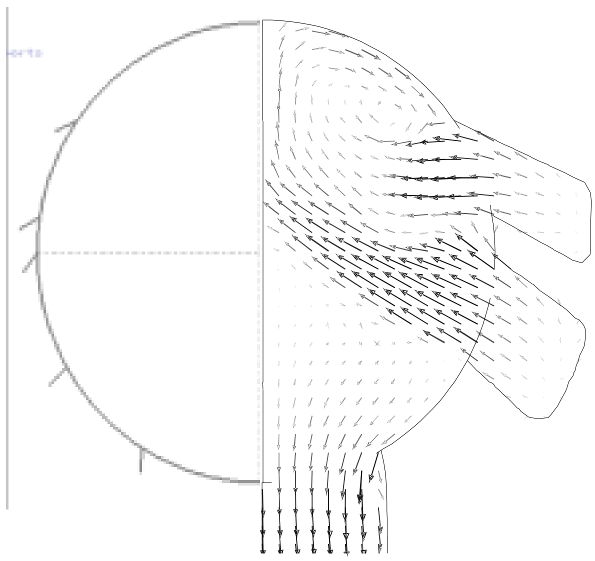

Figure 5: Flow field comparison CFD versus fired experiments, CFD results in a horizontal plane 4 mm above BDC, 180° a.t.d.c.

Results and discussion: Figure 6 shows the calculated total and fuel mass flux (“mixture”) in the exhaust. The integral of the lower curve represents the scavenge losses and thus the HC emissions. The upper curve represents the total fluid mass flow into the exhaust. At 102.5° a.t.d.c., the exhaust opens allowing the burned charge to expand into the muffler. At the end of blow-down period (125.3°), the transfer ports open. Approx. 42° later, the fuel mass flux curve (lower curve) rises. Commonly, this rise is regarded as indicating scavenge losses due to fuel short circuiting

over the piston. After completion of the expansion phase, the gas velocity in the exhaust decreases leading to a slight reduction in the fuel mass flux as well since the real fuel mass flux into the exhaust is the result of the velocity multiplied by the actual concentration of unburned hydrocarbons (see Figure 7).
Later in the scavenge process, the fuel mass flux rises again. The emissions in this phase and especially directly before exhaust closure depend highly on how the Schnürle loop penetrates through the combustion dome leaking into the exhaust. However, as already indicated by the flow images from the steady flow simulation above, there seems to exist a significant loss path not covered by these contemplation even though these results agree qualitatively well with those presented by [Sawada et al. 1998].

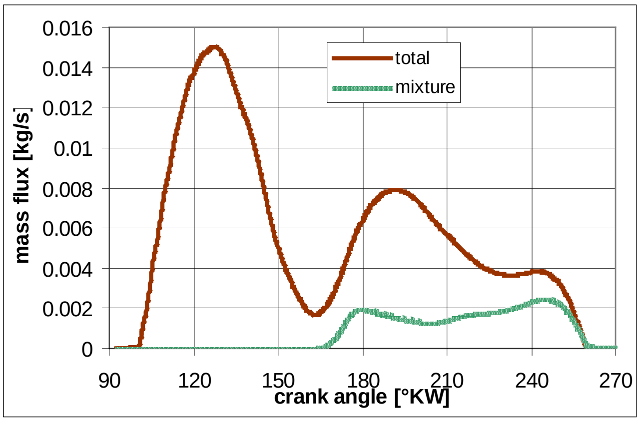

Figure 6: Fuel mass flux in the exhaust versus crankshaft angle over the scavenge cycle

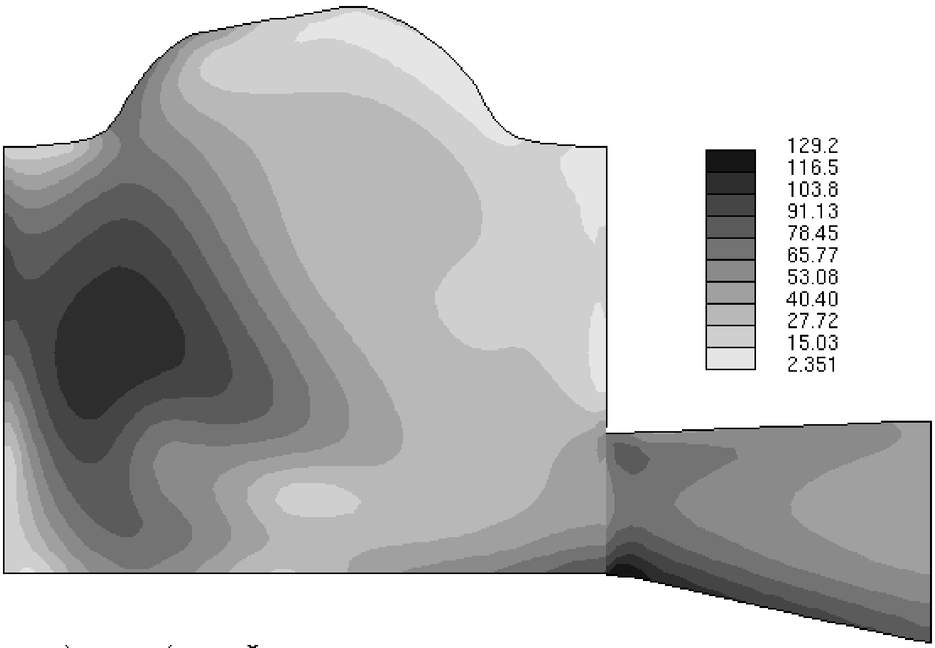

Figure 7: Scavenge loss represented by the product of concentration and velocity, approx. 190° a.t.d.c.

The results of the detailed loss mechanism analysis by means of the different balance cell surfaces now allow for a deeper insight into the origin of the scavenge losses during scavenging for the first time. Figure 8 presents the break-down of the total scavenge losses into the different paths. The exhaust opens at 102.5° a.t.d.c.. After about 30° crank angle delay, the rising black curve indicates direct mixture short-circuiting as the major loss path during the early scavenging period. At about 200 ° a.t.d.c., the Schnürle-loop losses clearly contribute most to the scavenge losses. In total, the Schnürle-loop losses result in 39% of the total losses. This can already be seen from Figure 7 where a high mass flux density within the Schnürle-loop in the combustion dome is present.
The near-wall secondary losses that are driven by the pressure difference as discussed below in the section “Driving Forces for the Near-Wall Secondary Losses”, result in a contribution of 15% of total scavenge losses which is only slightly less than the central mixing losses.
It is obvious that the precise figures of the loss contribution for the single paths depend to a certain extent on the definition of the balance cell surfaces. However, the general view on the process and the fact, that the near-wall secondary flow losses carry a significant of the scavenge losses remains valid.

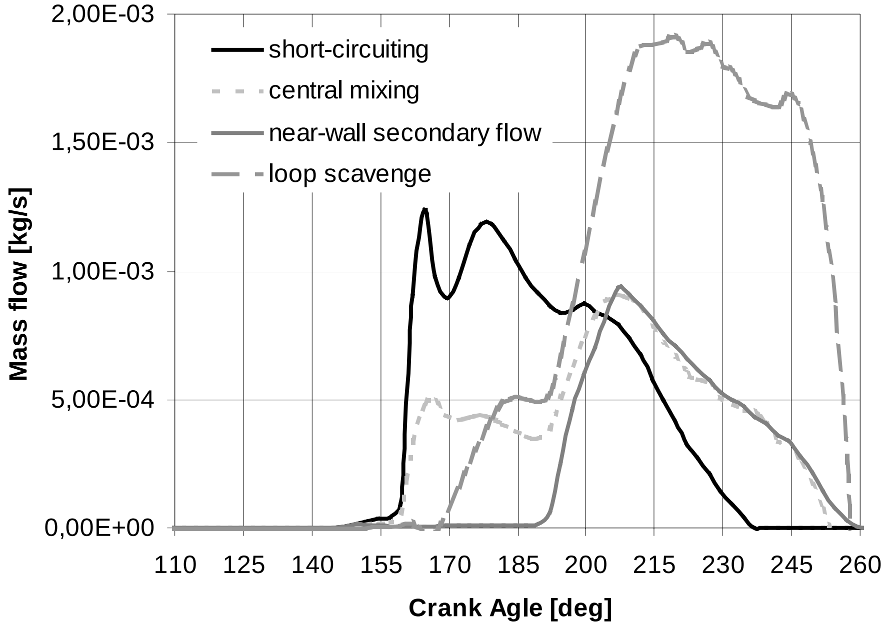

Figure 8: Characteristic of HC-loss mechanisms, w.o.t., 9000 rpm

Driving Forces for the Near-Wall Secondary Losses: The global balance clearly shows that a significant part of the scavenge losses creeps along the wall to the exhaust. This phenomenon may be described as a near wall (or even boundary layer) secondary flow. Those flow mechanisms are well known from turbine applications for example where the driving pressure difference between suction and pressure side within a flow channel induces a secondary flow in the boundary layers near the inner and outer radii of the flow channel.

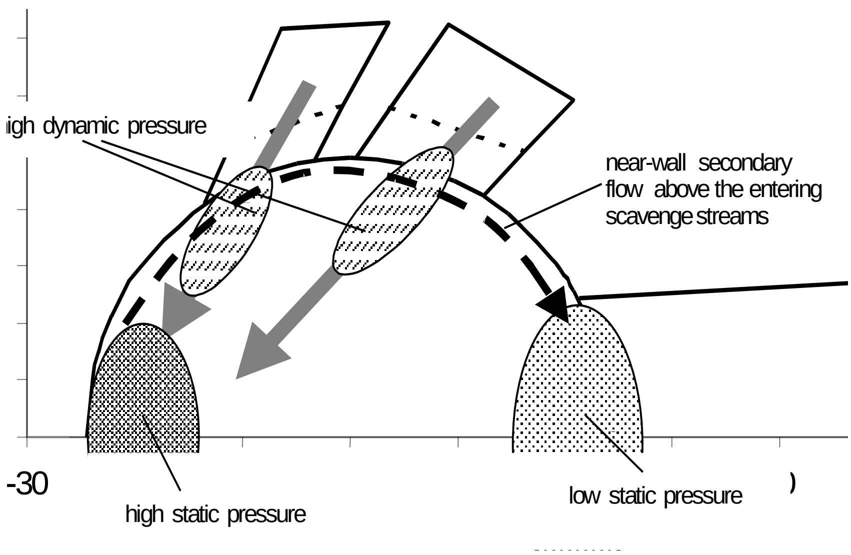

Figure 9: Static pressure distribution at different horizontal cylinder sections

A contemplation of the pressure situation within the cylinder clearly shows that the driving mechanisms are quite similar to the turbine secondary flows. Detailed analyses of the static pressure field within the cylinder in different sections at various cylinder height positions over the scavenge cycle show that a path of continuously decreasing static pressure exists near the wall between the area opposite the exhaust and the exhaust itself. Figure 9 presents a summarizing sketch of the pressure situation. In the region opposite to the exhaust, a high pressure area is visible. This high pressure area results from static pressure recovery: In the crankcase, the static pressure (which is basically the total pressure) of p_{cc} is given. The accelerating flow in the transfer ports yields a static pressure reduction ($p_{tot,cc}$-p_{dyn}). Within the ports and at the window, significant pressure losses apply so the entering scavenge stream has a static pressure level of $p_{stat,in}$ with a corresponding dynamic pressure according to the velocity. In the convergence zone at the inlet side, the fluid streams decelerate and the dynamic pressure partly recovers giving a static pressure p_1 (Figure 10) that is in average higher than the pressure in the near-wall region towards the exhaust and at the exhaust itself (p_2 in Figure 10).

In the core flow region (center of the cylinder volume and combustion dome) where the Schnürle-loop is formed, a pressure gradient resulting from streamline curvature keeps the balance to the driving pressure difference p_1-p_2 so that the loop is properly formed and almost no direct short-circuiting appears through the center of the volume.

In the near wall flow where the velocities are close to zero, there is no balancing pressure gradient present, so that the driving pressure gradient results in a convective transport of rich mixture towards the exhaust.

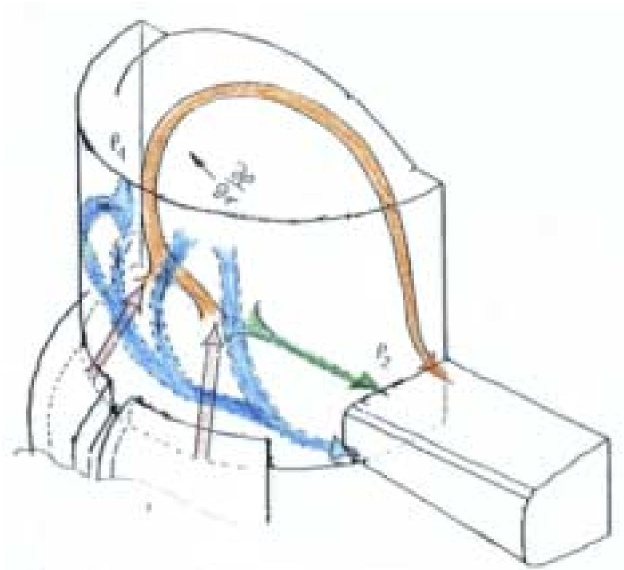

Figure 10: Scavenge loss paths and pressure situation within the cylinder

As major conclusion from these new findings may be drawn that the driving pressure difference and by this the portion of secondary flow losses may be controlled by a variation of entering scavenge flow momentum and plan angle layout. However, as variations from steady state simulations show there seems to exist a trade-off between Schnürle-loop-losses and secondary flow-losses. Further work is therefore necessary to exploit up to which extent these findings allow for new scavenge approaches to resolve this trade-off issue.

Conclusions: In the present study, four clearly distinguished loss mechanisms have been discussed: Direct mixture short-circuiting, late loop losses, central mixing losses and near-wall secondary flow losses. The results show that the newly identified near-wall secondary flow mechanism is of significant importance if an optimized port layout is to be developed. First computations show that there seems to exist a trade-off between the direct short-circuiting and the secondary flow losses. Steep plan angles for the scavenging ports that are directed towards the inlet side help in avoiding short circuiting but at the same time the secondary flow losses increase.

These near-wall secondary flow losses are also the most likely reason that stratified charging concepts that feature a four-port layout with a pair of transfer ports close to the exhaust that feed very lean mixture [Wolf 1977, Zahn et al. 2000], are limited in their emission reduction performance. The near wall secondary flows bypass the air curtain in the boundary layer.

Even though up to now, no general rule for an optimum balance between the different loss mechanisms has been presented, further research for reducing the engine out raw-emissions for Schnürle-scavenged engines is of major importance. Reduced raw emissions are the basis for successful catalyst concepts as well as for stratified scavenging designs. With the present results, a new view to the scavenge process is presented. The new understanding of the loss mechanisms will provide new opportunities to develop advanced scavenging concepts.

References:

Blair, G. P. (1996): Design and Simulation of Two-Stroke Engines, ISBN 1-56091-685-0, 1996

Morrison, K. (1998): *RedMax Certifies 2-Stroke Without Catalytic Muffler*, Power Equipment Trade, Vol. 20, Dec. 1998

Mugele, M., Tribulowski, J., Peters, H., Spicher, U., Rosskamp, H. (2001): *Numerical Analysis of Gas Exchange Processes in a Small Two-Stroke Gasoline Engine*, Paper submitted for SAE Fuels & Lubricants Meeting, San Antonio

Sawada, T.; Wada, Mi. (1998): *Development of a Low Emission Two-Stroke Cycle Engine*, SAE-Paper 980761

STAR CD Manuals (1997): Version 3.050A, Computational Dynamics Ltd. London

Wolf, F. (1977): Gemischgespülte Zweitakt-Brennkraftmaschine, German Patent No. DT2650834A1

Zahn, W., Rosskamp, H., Raffenberg, M., Klimmek, A. (2000): *Analysis of a Stratified Charging Concept for High-Performance Two-Stroke Engines*, SAE-Paper 2000-01-0900